Journal of Hunan University (Natural Sciences)

Vol. 52 No. 12
December 2025

Available online at
https://jonuns.com

Open Access Article https://doi.org/10.55463/issn.1674-2974.52.12.2

Optimizing Selective Overcurrent Protection in the IEEE 13-Node Feeder with Solar PV Using Micro Genetic Algorithm

Destra Andika Pratama[1*], Iwa Garniwa M.K[2], Abdul Halim[3]

[1,2,3] **Electrical Department, Universitas Indonesia, Depok, Indonesia**

* Corresponding author: destra.andika41@ui.ac.id

Article history
Received: November 7, 2025
Revised: December 14, 2025
Accepted: December 25, 2025
Published: January 30, 2026

Abstract: This study presents source-aware adaptive coordination of overcurrent protection for active distribution networks with distributed generation. The novelty of this study lies in the integration of source-relative time grading with IEC 60255-151 curve evaluation and the optimization of settings via a small-population micro-genetic algorithm that is evaluation-efficient, yet resistant to stagnation. The test system was an IEEE 13-node feeder hosting several photovoltaic units and a main grid, resulting in bidirectional fault currents. The objective is to ensure selectivity across on-grid (grid-connected) modes by enforcing a coordination time interval (CTI) of ≥ 0.40 s while minimizing the total operating time of the primary relays. These methods include MATLAB/Simulink modelling for low- and high-fault scenarios, and the operating times are computed using the IEC 60255-151 Inverse Curve. The Time Multiplier Settings (TMS) were tuned with a micro-GA (population = 20, iterations = 20, crossover probability = 0.8, mutation probability = 0.08), with elitism and a restart mechanism upon loss of diversity. The results show that across eight scenarios (A-H), all primary-backup pairs satisfy selectivity with a CTI not less than 0.40 s; near-threshold cases gain a 5 ms buffer without violating device limits. The tightest sensitivity margin occurred in Scenario F and the narrowest TMS headroom occurred in Scenario G, both of which were recommended as priority monitoring points. In conclusion, a coordination principle defined relative to the source in-feed, combined with auditable IEC curve formulations and low-cost optimization, yields selective, sensitive, and efficient designs. The principle generalizes to multisource active networks, given an M-ratio > 1, compliance with the TMS bounds, and current estimates aligned with the operating topology. Future work will include Monte Carlo robustness tests and co-optimization of TMS and pickup with relay-specific IEC curve selection, followed by HIL validation.

Keywords: Adaptive overcurrent protection; active distribution networks; distributed generation; micro-genetic algorithm (μGA); IEC 60255-151; coordination time interval (CTI).

基于微遗传算法的含光伏电源 IEEE 13 节点馈线选择性过流保护优化

摘要：本研究面向含分布式发电的有源配电网过流保护，提出一种源感知的自适应配合方案。其创新点在于将以电源为参照的时间分级与 IEC 60255-151 标准曲线评估相结合，并采用小种群微遗传算法（micro-GA）对继电器定值进行优化；该算法在评估效率较高的同时，对停滞和早熟收敛具有较强抑制能力。测试系统为 IEEE 13 节点馈线，接入若干光伏单元及主网电源，导致故障电流呈双向流动。研究目标是在并网运行模式下，通过强制协调时间间隔（coordination time interval，CTI）≥ 0.40 s，并尽可能缩短主保护继电器的总动作时间，以保证系统保护的整体选择性。方法上，首先在 MATLAB/Simulink 中分别构建低故障电流水平与高故障电流水平两类场景，并依据 IEC 60255-151 标准反时限曲线计算各继电器的动作时间；随后，利用带有精英保留机制及种群多样性丧失时重启机制的小种群 micro-GA 对时间倍数系数（time multiplier setting，TMS）进行整定（种群规模 = 20，迭代次数 = 20，交叉概率 = 0.8，变异概率 = 0.08）。结果表明，在 8 种运行场景（A-H）下，所有主-备保护对均满足选择性要求，CTI 均不小于 0.40 s；对于接近阈值的工况，在不违反装置极限约束的前提下，仍可获得 5 ms 的安全裕度。最紧的灵敏度裕度出现在场景 F，而最小的 TMS 裕度则出现在场景 G，因此这两类工况被建议作为优先监视点。综上，在以电源馈入为参照建立的保护配合原则下，结合可审计的 IEC 曲线解析形式与低成本优化方法，可实现选择性良好、灵敏度高且动作高效的过流保护设计；在满足 M 比率（M-ratio）> 1、TMS 取值服从边界约束且故障电流估计与实际运行拓扑一致的条件下，该原则可推广至多电源有源配电网络。后续工作将开展基于蒙特卡洛方法的鲁棒性测试，并在继电器特定 IEC 曲线选型的基础上，对 TMS 与整定电流进行联合优化，最终通过硬件在环（hardware-in-the-loop，HIL）试验完成验证。

关键词：自适应过流保护；有源配电网络；分布式发电；微遗传算法（μGA）；IEC 60255-151；协调时间间隔（CTI）.

1. Introduction

1.1. Background and Motivation

Power distribution systems are evolving from a single-source radial pattern to an active grid with a massive penetration of dispersed plants. This transformation is driven by the smart grid agenda and clean energy transition, which raises expectations for reliability, selectivity, and sensitivity at medium- and low-voltage levels [1], [2], [3], [4], [5], [6], [7], [8].

The presence of dispersed generators changes the network-operating profile, including the load current, power factor, and power flow direction. These changes have a direct impact on the magnitude and direction of the short-circuit current and location of the source that supplies the fault. Time and flow coordination, which were historically designed for a single dominant source of substations, became vulnerable when the system operated in a multisource state. This indicates the need for an adaptive and topology-aware protection strategy to maintain the validity of the settings when configuration and in-feed change [1], [2], [7], [8].

1.2. The Impact of Dispersed Power Plants on Conventional Protection

The presence of scattered generators modifies the location of the in-feed and the level of the short-circuit current; thus, the premise of coordination centered on the substation loses its validity in a number of scenarios [9], [10], [11], [12]. Empirical and simulated evidence reports decreased selectivity, the emergence of backflow, and undesirable disconnection events when multiple sources are simultaneously active.

The methodological response recommended in the literature is the application of overcurrent relays to bidirectional power flow as well as adaptive strategies to maintain selectivity in feeders rich in scattered generators [13], [14], [15], [16], [17], [18]. In this context, the term *bidirectional* refers to the fact that, once inverter-based photovoltaic (PV) units are connected to the feeder, the power and fault currents may flow in either direction along several line sections, depending on the operating mode and the in-feed mix. This paper focuses on such bidirectional network conditions while modelling only non-directional ANSI 51 overcurrent elements; directional elements 67/67N embedded in practical relays are intentionally kept disabled and remain outside the scope of this study.

These claims are supported by case studies of overcurrent relay coordination in networks with scattered plants, more adaptive current schemes in distribution networks, and coordination studies in network-connected modes. The research is focused on on-grid operations, whereas the islanded scheme is reserved for further work. All three show a consistent mechanism for enforcing selectivity when the sources and topologies change [16], [17], [18].

1.3. Related Works and Gaps

Adaptive and intelligent protection includes expert system approaches, neural network methods, and a wide range of more directional current coordination optimization formulations that utilize interval programming, integer linear programming, finite quadratic programming, and search techniques for various topologies and characteristics of relays [14], [15], [19], [20], [21]. In the realm of microgrids, the key work explicitly distinguishes between grid-connected and islanded modes and proposes a more adaptive current scheme that is resilient to changes in configuration and availability of dispersed plants [17], [18], [20]. In this study, it was limited to the on-grid mode.

The impact of scattered generation on selectivity in radial and mesh networks has been measured using coordination indices and topological detection mechanisms [22], [23]. Meanwhile, the issue of sympathetic disconnection and isolated events has become a recurring concern [24], [25]. However, many solutions in the literature are still snapshot-based or treat the two modes separately, such that they do not lock in a transition policy that follows multi-generation availability and still maintain selectivity relative to the source when the in-feed location shifts [17], [18], [19], [20], [22], [23], [24], [25].

1.4. Objectives and Contributions

This study proposes a more adaptive flow coordination strategy that is standard-aware and relative to the source of a distributed distribution system rich in scattered generation. This proposal departs from the need to maintain selectivity in the low and high fault current ranges and in the on-grid operating modes while maintaining the operating speed of the primary relay.

First, the availability of scattered generators is integrated into the setting policy that is updated in the network rather than as a fixed value in a single scenario [9], [10], [11], [12], [16], [19].

Second, the sequence from downstream to upstream is defined relative to the source supplying the fault, that is, the substation in the grid-connected mode and the conventional source [17], [18], [20], [25], [26].

Third, the coordination time interval is enforced at low and high fault current levels, while minimizing the primary relay operation time to achieve a balance between speed and selectivity [16], [19], [20], [21], [22].

Fourth, the proposed architecture is modular and scalable, such that it can be extended to multiple plant locations spread across standard and practical feeders, including IEEE 13-node [1], [26], [27].

All these objectives are designed to be directly connected to the formulation of methodologies and implementation in Section 2, as well as to the empirical results in Section 3. In Section 2, the test system, protection philosophy relative to the source, formulation of the curve according to IEC 60255 151, estimation of the short-circuit current, and optimization mechanism using the micro-genetic algorithm of a small population are described in detail. In Section 3, eight fault scenarios are used to evaluate the consistency of the fault current to the pickup current ratio, coordination time interval examination, and protection implications, including the addition of time buffers to a number of threshold relay pairs so that all results remain within the device limits and meet the selectivity requirements.

With this preparation, the introduction not only captures the engineering needs of the active network but also maps the causal chain from the operational profile to the coordination formulation that maintains the selectivity of the on-grid operations evaluated in this study. The connection between backgrounds, issues, gaps, and contributions is explicitly shown so that the flow of methods and results becomes transparent and traceable by the researcher.

2. Methods and Materials

2.1. Description of Test Systems and Topological Changes

The evaluation was performed on an IEEE 13-node test system based on 4.16 kV. This test system was chosen because it represents an unbalanced distribution network with diverse channel types and the presence of in-line power transformers, making it relevant to observe the effect of changing short-circuit currents on overcurrent coordination performance.

The base model contained a single 115 kV source modeled as an infinite bus through a substation transformer with a capacity of 5000 kVA, without the presence of scattered generators.

To emulate an active distribution network, a photovoltaic (PV) inverter-based generator is connected at bus 675. The existence of multiple sources results in a two-way short-circuit current in several segments. On this basis, an ANSI 51 type overcurrent relay that can sense flows from both directions is placed in the corridor that connects the main network with the scattered plant to maintain selectivity when the in-feed quantity shifts [16], [17], [26]. These 51 elements respond to the magnitude of current regardless of direction; directional elements 67/67N available in practical relays are not modelled or enabled in this study, in line with the scope of the paper and the focus on magnitude-based grading.

The dataset used is consistent with the official IEEE 13-node test system material, including a 5000 kVA substation transformer with a configuration of 115 kV Δ to 4.16 kV, resistance of 1%, and reactance of 8%, as well as a 500 kVA step-down transformer of 4.16 kV to 0.48 kV with a resistance of 1.1% and reactance of 2%. The point load table per node includes buses 634, 645, 646, 652, 671, 675, 692, and 611 [27].

The characteristics of dispersed generation technology are noted because the difference between an induction generator or doubly fed induction generator and a full inverter results in different fault current contribution limits as well as different control dynamics, which then affects the pickup sensitivity and relay coordination [10], [12], [18].

2.2. Protection Philosophy and Source-Relative Grading

The philosophy used in this study was time grading. The protection device that is electrically furthest from the source that provides the in-feed fault must first operate. The backup device on the upstream side operates after a certain time interval, defined as the coordination time interval. The sequence from downstream to upstream is defined relative to the source supplying the interrupt current at that time, that is, the substation when the system is connected to the main network or the plant is scattered [17], [18], [20], [26].

By mapping the sequence of operations to the actual fault current flow path in the running mode, selectivity is maintained when there is a change in topology or source feasibility, such that there is no presumption that the settings in one automatic mode are safe in another mode without relevant current verification.

2.3. Relay Characteristics and Setting Constraints

The relays follow the inverse curve equation according to IEC 60255-151, which includes the Standard Inverse, Very Inverse, Extremely Inverse, and Long-Time Inverse. The standard constants of the curve were 0.14, 13.5, 80, and 120 for the Standard Inverse, Very Inverse, 80 for the Extremely Inverse, and 120 for the Long-Time Inverse, respectively. The constant and shape of the curve are also described in the Network Protection and Automation Guide [31]. To ensure completeness, ANSI and IEEE define different types of curves in the IEEE C37.112 standard. In this study, the IEC curve was used to calculate the operating time [28].

For the fault current I_f relative to the pickup current I_s and the Time Multiplier Setting, the following operating time equation is used:

Standard Inverse; t = $TMS \times \frac{0.14}{\left[\left(\frac{I_f}{I_s}\right)^{0.02} - 1\right]}$

Very Inverse: t = $TMS \times \frac{13.5}{\left[\left(\frac{I_f}{I_s}\right) - 1\right]}$

Extremely Inverse: t = $TMS \times \frac{80}{\left[\left(\frac{I_f}{I_s}\right)^{2} - 1\right]}$

Long-Time Inverse: t = $TMS \times \frac{120}{\left[\left(\frac{I_f}{I_s}\right) - 1\right]}$

The following setting constraints were enforced: the pickup current was not less than the local maximum load current, and the Time Multiplier Setting value was within the limits of the device. For each primary and backup pair at the protection site, selectivity is enforced at two levels of fault current (low/high) in the network-connected mode (on-grid) provided that the backup operation time minus the primary operating time is not less than the value of the coordination time interval for the entire fault scenario. The set of scenarios included low and high fault currents in network-connected (on-grid) mode. This formulation is compatible with modern adaptive coordination and optimization studies [16], [19], [20], [21], [22], [28].

2.4. On-Grid Short-Circuit Estimation and Current Levels

For each line segment, the short-circuit current is calculated using Thevenin's equivalent approach viewed from each active source, that is, the main network and scattered generator. This approach is common in dispersed-generation impact and protection coordination studies [16], [19], [22].

Two current levels were used to represent the practical range. Low levels represent sensitive critical conditions such as remote locations, high impedances, or inverter-based sources with current restrictions. High levels represent conditions near strong sources that are critical for the equipment and coordination.

Network-connected mode occurs when the system is connected to the main network. The isolated mode occurs when the system detaches from the main network or a scattered generator acts as a local source [18], [20], [25]. The scope of the numerical evaluation reported in this study is limited to the network-connected mode (on-grid). Thus, the selection of grading rules relative to the source in Subsection 2.2, is directly tied to the mode of network connection and the estimated current in Subsection 2.4, thus forming a clear chain of cause and effect.

2.5. Adaptive Coordination Framework

The purpose of optimization is to determine the pickup current and Time Multiplier Setting of each overcurrent relay on a bidirectional power flow network such that the primary operating time is minimized, selectivity is maintained based on coordination time intervals, and all device limits are adhered to. Relay overcurrent coordination is commonly formulated as a constraint-bound optimization problem [17], [18], [19], [21].

The upstream data from Subsections 2.1-2.4 (topology, Thevenin equivalent, set of low/high current scenarios, primary-reserve pairs of relative-source ranking results) are the evaluation inputs so that the policy is aware of the source. The mode detection steps are listed for framework completeness, while the reported performance evaluations are on a grid [17], [18], [20].

The inputs of each evaluation cycle include flows, topology snapshots, and Thevenin equivalents per source. The outputs include a selection of curve types, current pairs of pickup currents, latest Time Multiplier Setting, indicators of coordination time interval violations, and readjustment recommendations.

The work steps consist of taking measurements, estimating short-circuit currents at low and high levels of each active source, compiling the classification of the protection path relative to the source to define the primary and backup relay pairs, and the optimization process to select the type of curve and pickup current pairs as well as the Time Multiplier Setting. Model mapping to integer linear programming or finite quadratic programming can be selected according to software and operational requirements [19], [21].

This architecture is consistent with adaptive protection practices on microgrids and multi-source existence [17], [18], [20] while absorbing modern coordination optimization techniques [19], [21], [22].

2.6. Micro Genetic Algorithm

A. Principle

A microgenetic algorithm was used as the optimization approach. Essentially, a Micro Genetic Algorithm is a small-population Genetic Algorithm equipped with a repeating mechanism to prevent genetic diversity from stopping at the local optimum. Krishnakumar introduced this small-population approach and named it a micro-genetic algorithm [29].

The main characteristics of the small-population approach are summarized in a reference stating that the Micro Genetic Algorithm develops very small populations and needs to be repeated when genetic diversity is lost. The rationale for this approach to relay coordination is that the evaluation of the objective function of the protection system is an expensive process because it includes a multi-scenario fault simulation, time flow curve calculation, and coordination time interval testing. A small population reduces the number of evaluations and accelerates convergence, noting that the risk of stagnation is overcome by repetition and adaptive mutations [30].

The workflow used follows the general pattern of the Micro Genetic Algorithm, namely, individual selection, cross-switching process with high chances, low-to-medium value mutations, evaluation of goal and constraint functions, and detection of stagnation to trigger repetition. The applied form of repetition retains the one to two best solutions as elite and reinitializes other individuals for diversity recovery. This pattern is consistent with the practice of small-population Genetic Algorithms in dynamic landscapes [31].

Parameters used: population size 20, maximum iteration of 20 generations, chance of cross-switching 0.8, chance of mutation 0.08, elitism of 1-2 best individuals saved on restart, restart criteria when there is no improvement of 5-10 generations or population variance drops below the threshold, representation of chromosomes as optional real vectors $[TMS_1, \ldots., TMS_{12}]$ aadds pickup for co-optimization), variable limits: TMS in the range of devices $I_s \geq I_{load\ maxs}$. The formulation of the objective functions is consistent with the DOCR coordination literature: minimizes the primary operating time by meeting the coordination constraints of the inverse curve constant following IEC 60255-151. Scope of evaluation: coordination time interval (CTI) penalties are evaluated in low/high-current scenarios in on-grid mode.

The formulation of the objective functions is consistent with that in the literature on directional overcurrent relay coordination. The main goal is to minimize the primary relay operation time while still satisfying the coordination constraints. Equivalent statements can be found in several sources, explaining that coordination problems set the pickup currents and time multipliers such that the operating time is minimized and coordination constraints are met [31], [32], [33].

The fitness function compiles the primary operating time and penalties for each violation of the coordination time interval. Penalties are imposed in such a way that violations become costly. With this construction, a viable and selective solution is always preferred over a quick one that violates the boundaries of coordination. The curve constant for the inverse curve follows IEC 60255-151, where k and α are as stated in the manufacturer's documentation and technical guidelines [34].

B. Implementation

A flowchart of the algorithm used to ensure adaptive relay coordination in the modified IEEE 13-node test system is shown in Figure 1. The algorithm is explained step-by-step as follows:

Step 1 Inputs & Constraints
Retrieve on-grid (low/high) fault current data, pickup limit, CTR, number of relays, primary-backup pairs, TMS limits, and CTI target ≥ 0.40 s.

Step 2 Model & Fitness Specification
Set the IEC 60255-151 curve per relay and define the fitness as This ensures that selectivity occur first. $\sum \text{primary operation time} + \text{big penalties for violations CTI/limit}$.

Step 3 Population Initialization
Generate a small population of TMS vectors within the limit; project value beyond the range; set gen = 1 and, $G_{max} = 20$.

Step 4 Evaluate Current Population
Calculate the primary-backup time for all pairs and current levels and save the CTI margin and fitness value.

Step 5 Selection Variation Evaluation
Tournament selection, *crossover* $p = 0.8$; mutation $p = 0{,}08$; project to the limit, evaluation of offspring with the procedure in Step 4.

Step 6 Survivors Convergence Restart/Stop
Elitism (1-2 best) was
- If there is no 5-10 generation fix or variant < threshold, restart the population (save elite) and gen++ then return to step 4.
- If gen > G_{max}, stop and proceed to validation.
- In addition, gen++ and return to step 4

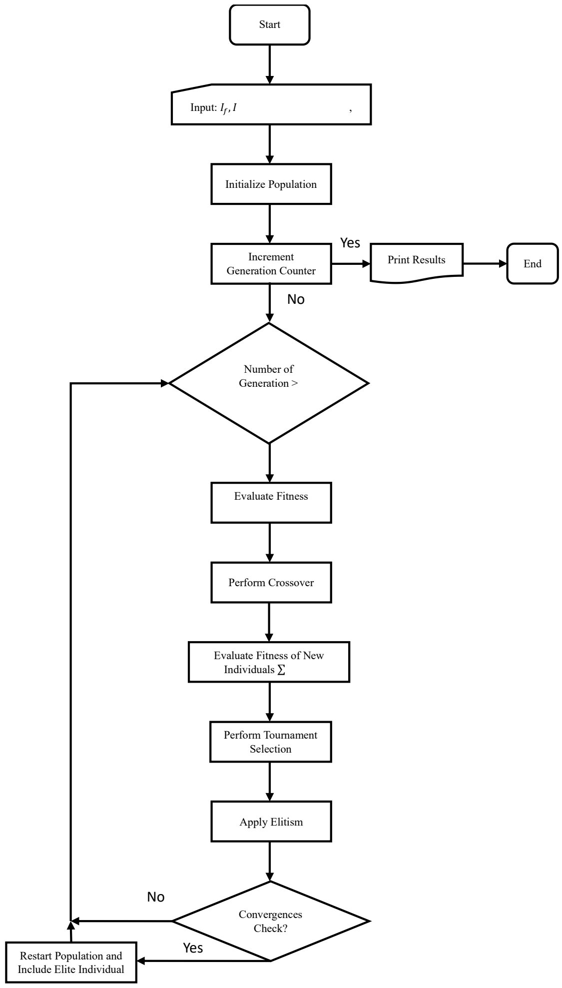

Figure 1. µGA for adaptive scheme

2.7. Test System Data

Table I. Transformer Data (IEEE 13-node) [27]

Transform	Power (kVA)	High Voltage (kV)	Low Voltage (kV)	R (%)	X (%)
Substation	5000	115-D	4.16-Gr. Y	1	8
Step-down	500	4.16-Gr. Y	0.48-Gr. Y	1.1	2

Table II. Load Data per Phase (kW/kVAr) [27]

Node -	Load Model	Phase-1 (kW/kVAr)	Phase-2 (kW/kVAr)	Phase-3 (kW/kVAr)
634	Y-PQ	160/110	120/90	120/90
645	Y-PQ	0/0	170/125	0/0
646	D-Z	0/0	230/132	0/0
652	Y-Z	128/86	0/0	0/0
671	D-PQ	385/220	385/220	385/220
675	Y-PQ	485/190	68/60	290/212
692	D-I	0/0	0/0	170/151
611	Y-I	0/0	0/0	170/80
-	Total	1158/606	973/627	1135/753

3. Results and Discussion

3.1. Technical Context and Basis of Calculation

Testing was conducted on eight A-H fault scenarios with constant play-and-backup pairs. The system architecture follows a series of simulations run in

MATLAB and Simulink, as shown in Figure 2. The circuit contains generating blocks, lines, loads, transformers, current and voltage measurements, and a protection logic that implements inverse-time overcurrent relays.

The curve used for the entire relay was the IEC 60255-151 Invers Curve, with the equation $t = TMS \cdot \frac{k}{M^{\alpha}-1}$, $M = \frac{I_f}{I_p} \geq 1$. This equation is the standard form of IEC for overcurrent relays. IEEE equivalents and other curve variations were defined in IEEE C37.112 [28]. The constant values for the inverse curves $k \; and \; \alpha$, are listed in the document referencing IEC 60255-151 [35].

In coordination practice, the coordination time interval (CTI) between relay pairs is usually chosen in the range of 0.25 s to 0.40 s. For modern systems that demand high selectivity, a conservative value of 0.40 s is often used as a lower limit target.

Based on this, all trip time evaluations in this section follow the inverse curve equation, with M calculated from the ratio of the fault current to the pick-up current $M = \frac{I_f}{I_p}$. For operational reliability, a 5 ms buffer was added to the scenario that was originally at the 0.40 s threshold, so that the CTI was effectively above the minimum limit.

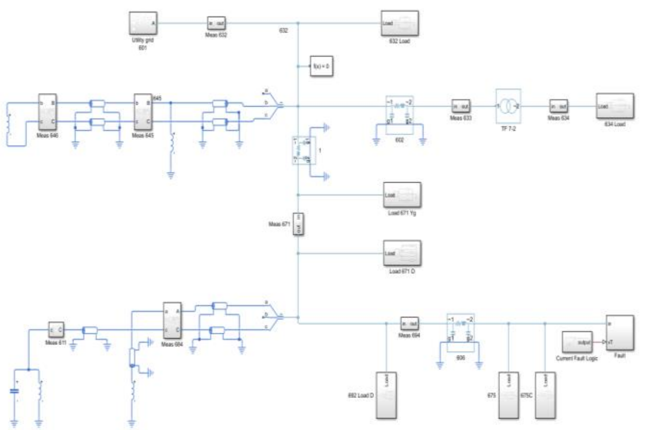

Figure 2. Adaptive protection and relay coordination scheme for Scenarios A-H.

The circuit shown in Figure 2 was used to generate a fault current at the point representing the protection path. The results of the current and voltage measurements on the relevant bus were then processed by the protection block to determine the relay operation times on the main and backup sides. Parameters I_f, I_p, TMS, M, and operating time are the inputs for the quantitative analysis in the next section.

A dedicated Nomenclature section is included in the manuscript to define all acronyms and symbols used in the text and, in particular, in Tables III–V, so that readers can interpret the numerical results without ambiguity. In the relay-coordination tables, the columns Flt, Main, and Bkp identify the simulated fault scenario and the associated main and backup relays. The quantities I_{p_m}(A) and I_{p_b}(A) denote the pickup current settings of the main and backup relays, whereas I_{f_m}(A) and I_{f_b}(A) are the corresponding fault currents seen by the main and backup relays in the short-circuit simulations. The dimensionless ratios M_m and M_{bkp} represent the multiples of pickup for the main and backup relays, defined as $M_m = I_{f\_m}/I_{p\_m}$ and $M_{\text{bkp}} = I_{f\_b}/I_{p\_b}$. In Tables IV and V, TMS_{main} and TMS_{Bpk} are the Time Multiplier Settings of the main and backup relays, while t_{main}(s) and t_{bkp}(s) denote their operating times computed from the inverse-time characteristic. The headings CTI and CTI results report, respectively, the coordination time interval between the main and backup relays and the value of this interval achieved for each primary-backup pair.

3.2. Basic Simulation Data

Tables III and IV present data for the eight disturbance scenarios.

Table III. Initial $I_p \; and \; I_f$ simulation results per scenario before buffer adjustments.

Flt	Main	Ip_m (A)	If_m (A)	M_m	Bkp	Ip_b (A)	If_b (A)	M_bkp
A	R1	89.9	7309	81.6	R2	89.4	7309	81.68
B	R2	197.2	8426	42.6	R3	627	8649	13.79
C	R4	84.4	3011	35.5	R5	84.7	3011	35.53
D	R6	84.4	3999	47.2	R7	93.8	3999	42.61
E	R8	93.5	3998	42.6	R7	93.8	3998	42.60
F	R10	789.0	7065	8.95	R9	509	997	1.96
G	R11	156.1	8487	54.35	R9	509	7065	13.87
H	R12	171.8	6288	36.60	R11	156	6287	40.25

Table IV. Initial $TMS \; and \; t$ simulation results per scenario before buffer adjustments.

Flt	Main	TMS_ Main	t_main (s)	Bkp	TMS_ bkp	t_bkp (s)	CTI results
A	R1	0.0500	0.0760	R2	0.3130	0.4760	0.40
B	R2	0.0500	0.0898	R3	0.1885	0.4898	0.40
C	R4	0.0500	0.0946	R5	0.2615	0.4946	0.40
D	R6	0.0500	0.0898	R7	0.2727	0.4898	0.40
E	R8	0.0500	0,0870	R7	0.4000	0.6958	0.61
F	R10	0.0500	0.1069	R9	0.1667	0.5069	0.40
G	R11	0.0543	0.1624	R9	0.3670	0.5624	0.40
H	R12	0.0500	0.0787	R11	0.3066	0.4787	0.40

Verification of the consistency of the M ratio shows that all rows are valid $M = \frac{I_f}{I_p} \geq 1$ for play and for backup. The most stringent sensitivity feasibility is for backup F with M equal to 1.96. In terms of CTI, five scenarios are at or above 0.40 seconds, while three scenarios (A, D, H) are right on the threshold due to millisecond rounding, potentially causing differences in interpretation if the compliance standard is read rigidly. The literature on coordination practice suggests the existence of a safe space a few milliseconds above the CTI limit to absorb the time resolution of the breaker and other uncertainties. Therefore, small adjustments were made to the backup TMS to form a 5 ms buffer.

3.3. Backup-TMS Adjustment for CTI Buffer

On the same curve the trip time is directly proportional to the TMS at a fixed value of M, and the TMS is only obtained through linear scaling, $TMS_{backup,new} = TMS_{backup,awal}, \frac{t_{main}+0{,}45}{t_{backup,awal}}$. The final result after adjustment is shown in Table V, with the new CTI at or above 0.405 s for scenarios previously at the threshold.

Table V. Final results after TMS adjustment for five-millisecond CTI buffers.

Flt	Main	TMS_ main	t_main (s)	Bkp	TMS_ bpk	t_bk p (s)	CTI results
A	R1	0.0500	0.076	R2	0.3163	0.481	0.405
B	R2	0.0500	0.089	R3	0.1884	0.489	0.400017
C	R4	0.0500	0.094	R5	0.2614	0.494	0.400033
D	R6	0.0500	0.089	R7	0.2754	0.494	0.405
E	R8	0.0500	0.087	R7	0.4	0.695	0.608822
F	R10	0.0500	0.106	R9	0.1683	0.511	0.405002
G	R11	0.0543	0.162	R9	0.367	0.562	0.40001
H	R12	0.0500	0.078	R11	0.3098	0.483	0.405001

All TMS values in Table V are within the range of 0.05-0.4. The smallest TMS headroom is in scenario G because the backup TMS is already 0.367 s, so the remaining space is 0.4 s narrower than in other scenarios. Scenario E remained unchanged because the initial CTI was well above 0.4 s, and the TMS was at the upper limit of 0.4. Overall, the minimum post-adjustment CTI was in the range of 0.40001 s (scenario G), and the average CTI increased from approximately 0.42610 s to 0.42861 s.

3.4. Technical Discussion and Protection Implications

The results in Table V are consistent with those obtained using the SI equation. The proportional relationship between the change in TMS and the change in trip time in M is in accordance with the IEC formulation [28], [35]. This validation is important because, in coordination studies, an undocumented mixture of IEC and IEEE curves can lead to bias in timing and CTI calculations. By holding one of the same curves for both relays, the coordination evaluation becomes deterministic and replicable.

Scenario F has a backup M of 1.96, which is the smallest margin of sensitivity. This value is still adequate but is most sensitive to changes in network operations, such as workstation variations, measurement deviations, or changes in the source impedance. If M decreases, the trip time increases according to the SI equation, which has the potential to affect the CTI of the downstream pair. This location is recommended for monitoring, and a contingency-setting profile is prepared.

The selection of 0.40 s as the lower limit of CTI is in line with the overcurrent device coordination guidelines, which recommend a minimum margin of 0.25-0.40 s between two protection devices to maintain selectivity at the relevant fault current range. The addition of a five-millisecond buffer in scenarios A, D, F, and H removed the ambiguity due to equipment rounding or time resolution without pushing the TMS out of the allowable range.

3.5. Simple Statistical Assessment

With eight scenarios, each with a pre- and post-buffer value pair, a simple statistical test is either a sign test or Wilcoxon signed-rank test on CTI differences. This does not require an assumption of normality. In these data, all CTI differences are positive; thus, they formally produce a small p-value in the sign test, and it can be concluded that the adjustment provides a statistically significant increase in the CTI. This claim is local in eight scenarios and is not intended to judge the superiority of one algorithm over another.

4. Conclusion

On the IEEE-13 bus, all primary-backup pairs achieved a coordination time interval of no less than 0.40 s after tuning the measured backup Time Multiplier Setting, with the addition of a five-millisecond buffer for scenarios that were at the threshold.

This principle is common for active networks with multi-infeed, as long as the M ratio remains above one, the Time Multiplier Setting limit is adhered to, and the short-circuit current estimation is performed consistently with the running topology.

Two edge conditions were identified: scenario F showed the smallest margin of sensitivity (the M ratio was close to the lower limit), whereas scenario G showed a narrow time-multiplier setting headroom. Both do not violate selectivity but become vulnerable points when system uncertainty increases; generalization to other topologies with extreme source impedances or specific generation characteristics requires additional verification.

A large population optimization method with high evaluation costs, a micro-genetic algorithm with an elite iteration and maintenance mechanism reduces evaluation costs without losing the quality of the solution in the Time Multiplier Setting continuous variable space, and pickup current when included

Theoretically, the results tie the IEC inverse curve to grading rules that are compatible with multiple sources, thereby forming an auditable analytical framework. In practical terms, this framework prescribes implementation: target coordination time intervals, realistic millisecond buffers, priority monitoring point assignment at locations with a low M ratio or narrow Time Multiplier Setting headroom, and replicable optimization-based tuning flows.

The following research suggestions are made: Recommended Monte Carlo-based resistance tests against variations in the current transformer ratio, source impedance, disconnect latency, and generation profile, systematic comparative studies with limited quadratic approaches, linear programming, and the expansion of the Time Multiplier Setting tuning to co-optimization of the Time Multiplier Setting and pickup current along with the selection of the IEC curve per relay.

Declarations

Funding
This research was supported by an Indonesian Education Scholarship, as well as institutional support from the Center for Higher Education Funding and Assessment, Ministry of Higher Education, Science, and Technology of the Republic of Indonesia, and the Endowment Fund for Education Agency, Ministry of Finance of the Republic of Indonesia.

Acknowledgements
The author expresses his appreciation for the sponsorship of the International Journal Publication to:
1. The Indonesian Education Scholarship.
2. Pusat Pelayanan Pembiayaan dan Asesmen Pendidikan Tinggi (Center for Higher Education Funding and Assessment), Ministry of Higher Education, Science, and Technology of Republic Indonesia.
3. Endowment Fund for Education Agency, Ministry of Finance of Republic Indonesia.

Conflicts of Interest
The author states that he has no financial or non-financial conflicts of interest related to this manuscript.

References

[1] P. P. Barker and R. W. D. Mello, "Determining the impact of distributed generation on power systems. I. Radial distribution systems," in *2000 Power Engineering Society Summer Meeting (Cat. No.00CH37134)*, 16-20 July 2000 2000, vol. 3, pp. 1645-1656 vol. 3, doi: 10.1109/PESS.2000.868775.

[2] R. C. Dugan and T. E. Mcdermott, "Distributed Generation: Operating Conflicts for Distributed Generation Interconnected with Utility Distribution Systems," *IEEE Industry Applications Magazine,* vol. 8, no. 2, pp. 19-25, 2002, doi: 10.1109/2943.985677.

[3] A. Battaglini, J. Lilliestam, A. Haas, and A. Patt, "Development of SuperSmart Grids for a more efficient utilisation of electricity from renewable sources," *Journal of Cleaner Production,* vol. 17, no. 10, pp. 911-918, 2009/07/01/ 2009, doi: https://doi.org/10.1016/j.jclepro.2009.02.006.

[4] J. A. Cardenas, L. Gemoets, J. H. Ablanedo Rosas, and R. Sarfi, "A literature survey on Smart Grid distribution: an analytical approach," *Journal of Cleaner Production,* vol. 65, pp. 202-216, 2014/02/15/ 2014, doi: https://doi.org/10.1016/j.jclepro.2013.09.019.

[5] P. D. Lund, J. Mikkola, and J. Ypyä, "Smart energy system design for large clean power schemes in urban areas," *Journal of Cleaner Production,* vol. 103, pp. 437-445, 2015/09/15/ 2015, doi: https://doi.org/10.1016/j.jclepro.2014.06.005.

[6] K. Hacatoglu, I. Dincer, and M. A. Rosen, "A new model to assess the environmental impact and sustainability of energy systems," *Journal of Cleaner Production,* vol. 103, pp. 211-218, 2015/09/15/ 2015, doi: https://doi.org/10.1016/j.jclepro.2014.06.050.

[7] S. A. M. Javadian, M. R. Haghifam, S. M. T. Bathaee, and M. Fotuhi Firoozabad, "Adaptive centralized protection scheme for distribution systems with DG using risk analysis for protective devices placement," *International Journal of Electrical Power & Energy Systems,* vol. 44, no. 1, pp. 337-345, 2013/01/01/ 2013, doi: https://doi.org/10.1016/j.ijepes.2012.07.056.

[8] K. Moslehi and R. Kumar, "A Reliability Perspective of the Smart Grid," *IEEE Transactions on Smart Grid,* vol. 1, no. 1, pp. 57-64, 2010, doi: 10.1109/TSG.2010.2046346.

[9] S. M. Brahma and A. A. Girgis, "Development of adaptive protection scheme for distribution systems with high penetration of distributed generation," *IEEE Transactions on Power Delivery,* vol. 19, no. 1, pp. 56-63, 2004, doi: 10.1109/TPWRD.2003.820204.

[10] J. Ma, X. Wang, Y. Zhang, Q. Yang, and A. G. Phadke, "A novel adaptive current protection scheme for distribution systems with distributed generation," *International Journal of Electrical Power & Energy Systems,* vol. 43, no. 1, pp. 1460-1466, 2012/12/01/ 2012, doi: https://doi.org/10.1016/j.ijepes.2012.07.024.

[11] K. Kauhaniemi and L. Kumpulainen, "Impact of distributed generation on the protection of distribution networks," in *2004 Eighth IEE International Conference on Developments in Power System Protection*, 5-8 April 2004 2004, vol. 1, pp. 315-318 Vol.1, doi: 10.1049/cp:20040126.

[12] N. Rezaei and M. R. Haghifam, "Protection scheme for a distribution system with distributed generation using neural networks," *International Journal of Electrical Power & Energy Systems,* vol. 30,

no. 4, pp. 235-241, 2008/05/01/ 2008, doi: https://doi.org/10.1016/j.ijepes.2007.07.006.

[13] S. A. A. Shahriari, A. Y. Varjani, and M. R. Haghifam, "Cost reduction of distribution network protection in presence of distributed generation using optimized fault current limiter allocation," *International Journal of Electrical Power & Energy Systems,* vol. 43, no. 1, pp. 1453-1459, 2012/12/01/ 2012, doi: https://doi.org/10.1016/j.ijepes.2012.06.071.

[14] K. Tuitemwong and S. Premrudeepreechacharn, "Expert system for protection coordination of distribution system with distributed generators," *International Journal of Electrical Power & Energy Systems,* vol. 33, no. 3, pp. 466-471, 2011/03/01/ 2011, doi: https://doi.org/10.1016/j.ijepes.2010.10.009.

[15] M. Singh, B. K. Panigrahi, A. R. Abhyankar, and S. Das, "Optimal coordination of directional over-current relays using informative differential evolution algorithm," *Journal of Computational Science,* vol. 5, no. 2, pp. 269-276, 2014/03/01/ 2014, doi: https://doi.org/10.1016/j.jocs.2013.05.010.

[16] W. El-khattam and T. S. Sidhu, "Resolving the impact of distributed renewable generation on directional overcurrent relay coordination: a case study," *IET Renewable Power Generation,* vol. 3, no. 4, pp. 415-425, 2009/12/07 2009, doi: 10.1049/iet-rpg.2008.0015.

[17] F. Coffele, C. Booth, and A. Dyśko, "An Adaptive Overcurrent Protection Scheme for Distribution Networks," *IEEE Transactions on Power Delivery,* vol. 30, no. 2, pp. 561-568, 2015, doi: 10.1109/TPWRD.2013.2294879.

[18] W. K. A. Najy, H. H. Zeineldin, and W. L. Woon, "Optimal Protection Coordination for Microgrids With Grid-Connected and Islanded Capability," *IEEE Transactions on Industrial Electronics,* vol. 60, no. 4, pp. 1668-1677, 2013, doi: 10.1109/TIE.2012.2192893.

[19] A. S. Noghabi, H. R. Mashhadi, and J. Sadeh, "Optimal Coordination of Directional Overcurrent Relays Considering Different Network Topologies Using Interval Linear Programming," *IEEE Transactions on Power Delivery,* vol. 25, no. 3, pp. 1348-1354, 2010, doi: 10.1109/TPWRD.2010.2041560.

[20] L. Che, M. E. Khodayar, and M. Shahidehpour, "Adaptive Protection System for Microgrids: Protection practices of a functional microgrid system," *IEEE Electrification Magazine,* vol. 2, no. 1, pp. 66-80, 2014, doi: 10.1109/MELE.2013.2297031.

[21] V. A. Papaspiliotopoulos, G. N. Korres, and N. G. Maratos, "A Novel Quadratically Constrained Quadratic Programming Method for Optimal Coordination of Directional Overcurrent Relays," *IEEE Transactions on Power Delivery,* vol. 32, no. 1, pp. 3-10, 2017, doi: 10.1109/TPWRD.2015.2455015.

[22] H. H. Zeineldin, Y. A. R. I. Mohamed, V. Khadkikar, and V. R. Pandi, "A Protection Coordination Index for Evaluating Distributed Generation Impacts on Protection for Meshed Distribution Systems," *IEEE Transactions on Smart Grid,* vol. 4, no. 3, pp. 1523-1532, 2013, doi: 10.1109/TSG.2013.2263745.

[23] M. S. Sachdev, T. S. Sidhu, and B. K. Talukdar, "Topology detection for adaptive protection of distribution networks," in *Proceedings 1995 International Conference on Energy Management and Power Delivery EMPD '95*, 21-23 Nov. 1995 1995, vol. 1, pp. 445-450 vol.1, doi: 10.1109/EMPD.1995.500768.

[24] S. P. Chowdhury, S. Chowdhury, C. F. Ten, and P. A. Crossley, "Islanding operation of distributed generators in active distribution networks," in *2008 43rd International Universities Power Engineering Conference*, 1-4 Sept. 2008 2008, pp. 1-5, doi: 10.1109/UPEC.2008.4651556.

[25] P. Mahat, Z. Chen, B. Bak-Jensen, and C. L. Bak, "A Simple Adaptive Overcurrent Protection of Distribution Systems With Distributed Generation," *IEEE Transactions on Smart Grid,* vol. 2, no. 3, pp. 428-437, 2011, doi: 10.1109/TSG.2011.2149550.

[26] Y. Ates, M. Uzunoglu, A. Karakas, A. R. Boynuegri, A. Nadar, and B. Dag, "Implementation of adaptive relay coordination in distribution systems including distributed generation," *Journal of Cleaner Production,* vol. 112, pp. 2697-2705, 2016/01/20/ 2016, doi: https://doi.org/10.1016/j.jclepro.2015.10.066.

[27] D. T. Feeders, "IEEE PES Distribution System Analysis Subcommittee's, Distribution Test Feeder Working Group," *ed,* 2013.

[28] G. Benmouyal *et al.*, "IEEE standard inverse-time characteristic equations for overcurrent relays," *IEEE Transactions on Power Delivery,* vol. 14, no. 3, pp. 868-872, 1999.

[29] K. Kalmanje, "Micro-Genetic Algorithms For Stationary And Non-Stationary Function Optimization," in *Proc.SPIE*, 1990, vol. 1196, pp. 289-296, doi: 10.1117/12.969927. [Online]. Available: https://doi.org/10.1117/12.969927

[30] R. Landa, D. Tovias-Alanis, and G. Toscano, "Optimization of Deep Neural Networks Using a Micro Genetic Algorithm," *AI*, vol. 5, no. 4, pp. 2651-2679doi: 10.3390/ai5040127.

[31] D. Saha, A. Datta, and P. Das, "Optimal coordination of directional overcurrent relays in power systems using Symbiotic Organism Search Optimisation technique," *IET Generation, Transmission & Distribution,* vol. 10, no. 11, pp. 2681-2688, 2016/08/01 2016, doi: https://doi.org/10.1049/iet-gtd.2015.0961.

[32] A. S. Noghabi, J. Sadeh, and H. R. Mashhadi, "Considering Different Network Topologies in Optimal Overcurrent Relay Coordination Using a Hybrid GA," *IEEE Transactions on Power Delivery,* vol. 24, no. 4, pp. 1857-1863, 2009, doi: 10.1109/TPWRD.2009.2029057.

[33] T. Foqha *et al.*, "Optimal Coordination of Directional Overcurrent Relays Using Hybrid Firefly–

Genetic Algorithm," *Energies*, vol. 16, no. 14, doi: 10.3390/en16145328.
[34] H. Leite, J. Barros, and V. Miranda, "The evolutionary algorithm EPSO to coordinate directional overcurrent relays," in *10th IET International Conference on Developments in Power System Protection (DPSP 2010). Managing the Change*, 29 March-1 April 2010 2010, pp. 1-5, doi: 10.1049/cp.2010.0318.
[35] C. Body, "International electrotechnical commission," 2018.

参考

[1] P. P. Barker 和 R. W. D. Mello，“确定分布式发电对电力系统的影响。I. 径向配电系统“，2000 年电力工程学会夏季会议（Cat.No.00CH37134），2000 年 7 月 16-20 日，2000 年，第 3 卷，第 1645-1656 页，第 3 卷，doi：10.1109/PESS.2000.868775。
[2] R. C. Dugan 和 T. E. Mcdermott，“分布式发电：与公用事业配电系统互连的分布式发电的运行冲突”，IEEE 工业应用杂志，第 8 卷，第 2 期，第 19-25 页，2002 年，doi：10.1109/2943.985677。
[3] A. Battaglini、J. Lilliestam、A. Haas 和 A. Patt，“开发超级智能电网以更有效地利用可再生能源电力”，《清洁生产杂志》，第 17 卷，第 10 期，第 911-918 页，2009/07/01/ 2009，doi：https://doi.org/10.1016/j.jclepro.2009.02.006。
[4] J. A. Cardenas， L. Gemoets， J. H. Ablanedo Rosas， and R. Sarfi， “A literature survey on Smart Grid distribution： an analytical approach，” Journal of Cleaner Production， vol. 65， pp. 202-216， 2014/02/15/ 2014， doi：https://doi.org/10.1016/j.jclepro.2013.09.019.
[5] P. D. Lund， J. Mikkola， and J. Ypyä， “Smart energy system design for large clean power schemes in urban areas，” Journal of Cleaner Production， vol. 103， pp. 437-445， 2015/09/15/ 2015， doi：https://doi.org/10.1016/j.jclepro.2014.06.005.
[6] K. Hacatoglu、I. Dincer 和 MA Rosen，“评估能源系统环境影响和可持续性的新模型”，《清洁生产杂志》，第 103 卷，第 211-218 页，2015/09/15/2015，doi：https://doi.org/10.1016/j.jclepro.2014.06.050。
[7] S. A. M. Javadian， M. R. Haghifam， S. M. T. Bathaee， and M. Fotuhi Firoozabad， “Adaptive centralized protection scheme for distribution systems with DG using risk analysis for protection devices placement，” International Journal of Electrical Power &&& Energy Systems， Vol. 44， no. 1， pp. 337-345， 2013/01/01/ 2013， DOI：https://doi.org/10.1016/j.ijepes.2012.07.056.
[8] K. Moslehi 和 R. Kumar，“智能电网的可靠性视角”，IEEE 智能电网汇刊，第 1 卷，第 1 期，第 57-64 页，2010 年，doi：10.1109/TSG.2010.2046346。
[9] S. M. Brahma 和 A. A. Girgis，“为分布式发电高渗透率的配电系统开发自适应保护方案”，IEEE Transactions on Power Delivery，第 19 卷，第 1 期，第 56-63 页，2004 年，doi：10.1109/TPWRD.2003.820204。
[10] J. 马， X. Wang， Y. Zhang， Q. Yang， and A. G. Phadke， “A novel adaptive current protection scheme for distribution systems with distributed generation，” International Journal of Electrical Power & Energy Systems， Vol. 43， no. 1， pp. 1460-1466， 2012/12/01/ 2012， doi: https://doi.org/10.1016/j.ijepes.2012.07.024.
[11] K. Kauhaniemi 和 L. Kumpulainen，“分布式发电对配电网络保护的影响”，2004 年第八届 IEE 电力系统保护发展国际会议，2004 年 4 月 5-8 日，2004 年，第 1 卷，第 315-318 页，第 1 卷，doi：10.1049/cp：20040126。
[12] N. Rezaei 和 M. R. Haghifam，“使用神经网络的分布式发电配电系统的保护方案”，《国际电力与能源系统杂志》，第 30 卷，第 4 期，第 235-241 页，2008/05/01/2008，doi：https://doi.org/10.1016/j.ijepes.2007.07.006。
[13] S. A. A. Shahriari， A. Y. Varjani， and M. R. Haghifam， “Cost reduction of distribution network protection in presence of distributed generation using optimized fault current limiter allocation，” International Journal of Electrical Power &&& Energy Systems， Vol. 43， no. 1， pp. 1453-1459， 2012/12/01/ 2012， doi：https://doi.org/10.1016/j.ijepes.2012.06.071.
[14] K. Tuitemwong 和 S. Premrudeepreechacharn，“配电系统与分布式发电机的保护协调专家系统”，《国际电力与能源系统杂志》，第 33 卷，第 3 期，第 466-471 页，2011 年 3 月 1 日，doi：https://doi.org/10.1016/j.ijepes.2010.10.009。
[15] M. Singh、B. K. Panigrahi、A. R. Abhyankar 和 S. Das，“使用信息差分演化算法优化定向过流继电器的最佳协调”，《计算科学杂志》，第 5 卷，第 2 期，第 269-276 页，2014 年 3 月 1 日，2014 年 DOI：https://doi.org/10.1016/j.jocs.2013.05.010。
[16] W. El-khattam 和 TS Sidhu，“解决分布式可再生能源发电对定向过流继电器协调的影响：案例研究”，IET Renewable Power Generation，第 3 卷，第 4 期，第 415-425 页，2009/12/07 2009，doi：10.1049/iet-rpg.2008.0015。

[17] F. Coffele、C. Booth 和 A. Dyśko，“配电网络的自适应过流保护方案”，IEEE Transactions on Power Delivery，第 30 卷，第 2 期，第 561-568 页，2015 年，doi：10.1109/TPWRD.2013.2294879。

[18] W. K. A. Najy、H. H. Zeineldin 和 W. L. Woon，“具有并网和孤岛能力的微电网的最佳保护协调”，IEEE 工业电子学刊，第 60 卷，第 4 期，第 1668-1677 页，2013 年，doi：10.1109/TIE.2012.2192893。

[19] A. S. Noghabi、H. R. Mashhadi 和 J. Sadeh，“使用区间线性规划考虑不同网络拓扑的定向过流继电器的最佳协调”，IEEE Transactions on Power Delivery，第 25 卷，第 3 期，第 1348-1354 页，2010 年，doi：10.1109/TPWRD.2010.2041560。

[20] L. Che、M. E. Khodayar 和 M. Shahidehpour，“微电网的自适应保护系统：功能微电网系统的保护实践”，IEEE 电气化杂志，第 2 卷，第 1 期，第 66-80 页，2014 年，doi：10.1109/MELE.2013.2297031。

[21] V. A. Papaspiliotopoulos、G. N. Korres 和 N. G. Maratos，“一种用于定向过流继电器最佳协调的新型二次约束二次规划方法”，IEEE Transactions on Power Delivery，第 32 卷，第 1 期，第 3-10 页，2017 年，doi：10.1109/TPWRD.2015.2455015。

[22] H. H. Zeineldin, Y. A. R. I. Mohamed, V. Khadkikar, and V. R. Pandi, “A Protection Coordination Index for Evaluating Distributed Generation Impacts on Protection for Meshed Distribution Systems ”, IEEE Transactions on Smart Grid, vol. 4, no. 3, pp. 1523-1532, 2013, doi：10.1109/TSG.2013.2263745.

[23] M. S. Sachdev、T. S. Sidhu 和 B. K. Talukdar，“用于配电网络自适应保护的拓扑检测”，载于 Proceedings 1995 International Conference on Energy Management and Power Delivery EMPD '95,1995 年 11 月 21-23 日，1995 年，第 1 卷，第 445-450 页，第 1 卷，doi：10.1109/EMPD.1995.500768。

[24] S. P. Chowdhury, S. Chowdhury, C. F. Ten, and P. A. Crossley, “Islanding operation of distributed generators in active distribution networks, ” in 2008 43rd International Universities Power Engineering Conference, 1-4 Sept. 2008, pp. 1-5, doi： 10.1109/UPEC.2008.4651556.

[25] P. Mahat、Z. Chen、B. Bak-Jensen 和 C. L. Bak，“分布式发电配电系统的简单自适应过流保护”，IEEE 智能电网汇刊，第 2 卷，第 3 期，第 428-437 页，2011 年，doi：10.1109/TSG.2011.2149550。

[26] Y. Ates、M. Uzunoglu、A. Karakas、A. R. Boynuegri、A. Nadar 和 B. Dag，“在包括分布式发电在内的配电系统中实现自适应继电协调”，《清洁生产杂志》，第 112 卷，第 2697-2705 页，2016 年 1 月 20 日，DOI：https://doi.org/10.1016/j.jclepro.2015.10.066。

[27] DT Feeders，“IEEE PES 配电系统分析小组委员会，配电测试馈线工作组”，以及 2013 年。

[28] G. Benmouyal 等人，“IEEE 标准过流继电器逆时间特性方程”，IEEE Transactions on Power Delivery，第 14 卷，第 3 期，第 868-872 页，1999 年。

[28] G. Benmouyal 等人，“IEEE 标准过流继电器逆时间特性方程”，IEEE Transactions on Power Delivery，第 14 卷，第 3 期，第 868-872 页，1999 年。

[29] K. Kalmanje，“用于稳态和非稳态函数优化的微遗传算法”，载于 Proc.SPIE，1990 年，第 1196 卷，第 289-296 页，doi：10.1117/12.969927。[在线]。可用：https://doi.org/10.1117/12.969927

[30] R. Landa、D. Tovias-Alanis 和 G. Toscano，“使用微遗传算法优化深度神经网络”，TO，第 5 卷，第 4 期，第 2651-2679doi：10.3390/ai5040127。

[31] D. Saha、A. Datta 和 P. Das，“使用共生生物搜索优化技术在电力系统中定向过流继电器的最佳协调”，IET Generation, Transmission and Distribution，第 10 卷，第 11 期，第 2681-2688 页，2016/08/01,2016，doi：https://doi.org/10.1049/iet-gtd.2015.0961。

[32] A. S. Noghabi、J. Sadeh 和 H. R. Mashhadi，“使用混合 GA 在最佳过流继电协调中考虑不同的网络拓扑”，IEEE Transactions on Power Delivery，第 24 卷，第 4 期，第 1857-1863 页，2009 年，doi：10.1109/TPWRD.2009.2029057。

[33] T. Foqha等人，“使用混合萤火虫-遗传算法优化定向过流继电器”，《能源》，第16卷，第14期，DOI：10.3390/EN16145328。

[34] H. Leite、J. Barros 和 V. Miranda，“协调定向过流继电器的进化算法 EPSO”，第 10 届 IET 电力系统保护发展国际会议 （DPSP 2010）。管理变

革，2010 年 3 月 29 日至 4 月 1 日 2010 年，第 1-5 页，doi：10.1049/cp.2010.0318。

[35] C. Body，“国际电工委员会”，2018 年。

Manuscript Information
Word count: 8,157 words (excluding references).

Peer-Review Record
Fast-track status: Not fast-tracked.
First-round reviews received: 3 reports.
Revision cycles completed: 3 rounds.
Final version submitted: December 25, 2025